Electronic Supplementary Material (ESI) for Journal of Materials Chemistry C.

Supporting Information

Air-stable n-channel organic field-effect transistors based on charge-transfer complexes including dimethoxybenzothienobenzothiophene and tetracyanoquinodimethane derivatives

Toshiki Higashino, Masaki Dogishi, Tomofumi Kadoya, Ryonosuke Sato, Tadashi Kawamoto and Takehiko Mori**

Synthesis

Nuclear magnetic resonance spectra were obtained in deuterated chloroform with a JEOL JNM-AL300 spectrometer operated at 300 MHz. EI-MS spectra were obtained on a JEOL JMS-QI050GC Ultra Quad GC/MS spectrometer.

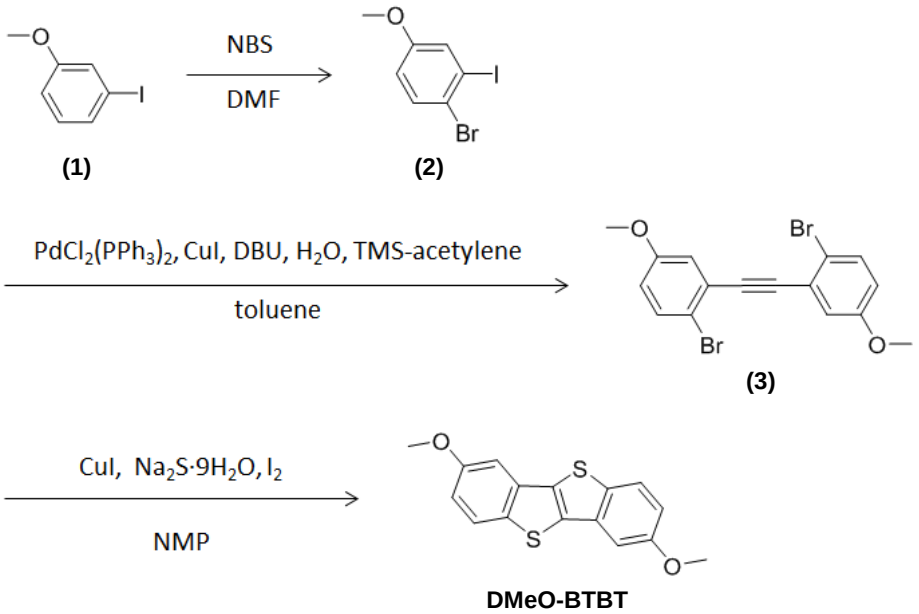

(1) **(2)** **(3)** **DMeO-BTBT**

3-Bromo-2-iodoanisole (2). This reaction was carried out under the ambient atmosphere in the dark. To a DMF solution (30mL) of 3-iodoanisole (**1**) (10.0 g, 42.7 mmol) was added *N*-bromosuccinimide (8.36 g, 47.0 mmol), and the mixture was stirred for 4 hours at 80°C. After cooling, the solution was poured into water, and extracted with diethyl ether. The organic phase was washed with saturated aqueous Na_2SO_3, water, and brine, and dried over $MgSO_4$. The evaporation of the solvent gave a yellow oil, which was subjected to column chromatography on silica gel eluted with dichloromethane-hexane (1:1, v/v). The product was obtained as a pale yellow oil (13.4 g, 42.7 mmol, yield 99%). Mass *m/z* 314 $[M+2]^+$, 312 $[M]^+$; ^{1}H-NMR ($CDCl_3$) δ = 3.77 (s, 3H), 6.77 (d, *J* = 8.8 Hz, 1H), 7.39 (s, 1H), 7.48 (d, *J* = 8.8 Hz, 1H).

1,2-Bis(2-bromo-5-methoxyphenyl)acetylene (3). This reaction was carried out under an argon atmosphere. To a solution of **2** (9.50 g, 30.4 mmol) in toluene (130 mL) was added powdered $PdCl_2(PPh_3)_2$ (1.36g, 1.92 mmol), CuI (0.60 g, 3.20 mmol), DBU (1,8-diazabicyclo[5.4.0]undec-7-ene) (28.8 mL, 192 mmol), H_2O (0.23 mL, 12.8 mmol), and trimethylsilylacetylene (2.2 mL, 16 mmol). The mixture was stirred for 18 hours at 60°C. After cooling, the solution was poured into water, and filtered by using Celite. The filtrate was extracted with diethyl ether, washed with H_2O, saturated aqueous NH_4Cl, and brine, and dried over $MgSO_4$. After evaporation of the solvent, the crude product was subjected to column chromatography on silica gel eluted with dichloromethane-hexane (1:3, v/v). The crude product was recrystallized from ethanol to give white crystals (3.87g, 9.77 mmol, yield 65%). Mass *m/z* 398 $[M+4]^+$, 396 $[M+2]^+$, 394 $[M]^+$; ^{1}H-NMR ($CDCl_3$) δ = 3.82 (s, 3H), 6.79 (d, *J* = 8.9 Hz, 1H), 7.14 (s, 1H), 7.49 (d, *J* = 8.9 Hz, 1H).

DMeO-BTBT (3,8-Dimethoxy-[1]benzothieno[3,2-*b*][1]benzothiophene). This reaction was carried out under an argon atmosphere. To a solution of **3** (4.49 g, 11.3 mmol) in refluxing NMP (*N*-methylpyrrolidone) (100 mL) was added CuI (0.430 g, 2.27 mmol), I_2 (5.76 g, 22.7 mmol), and $Na_2S \cdot 9H_2O$ (10.9 g, 45.4 mmol). The mixture was stirred for 48 hours at 120°C. After cooling, the solution was poured into water, extracted with ethyl acetate, and washed with brine. The evaporation of the solvent gave a white solid, which was washed with methanol and cooled acetone. The crude product was recrystallized from ethyl acetate to give yellow crystals (0.73 g, 2.4 mmol, yield 21%). Mass *m/z* 300 $[M]^+$; ^{1}H-NMR ($CDCl_3$) δ = 3.94 (s, 3H), 7.05 (d, J = 8.8 Hz, 1H), 7.30 (s, 1H), 7.05 (d, J = 8.8 Hz, 1H).

Optical properties

UV-Vis spectra of a 10^{-5} M chloroform solution was collected on a Shimadzu UV spectrophotometer 1800. The energy gap between HOMO and LUMO energy levels was calculated as E_g = 3.4 eV from the absorption edge with the wavelength of λ_{edge} = 360 nm.

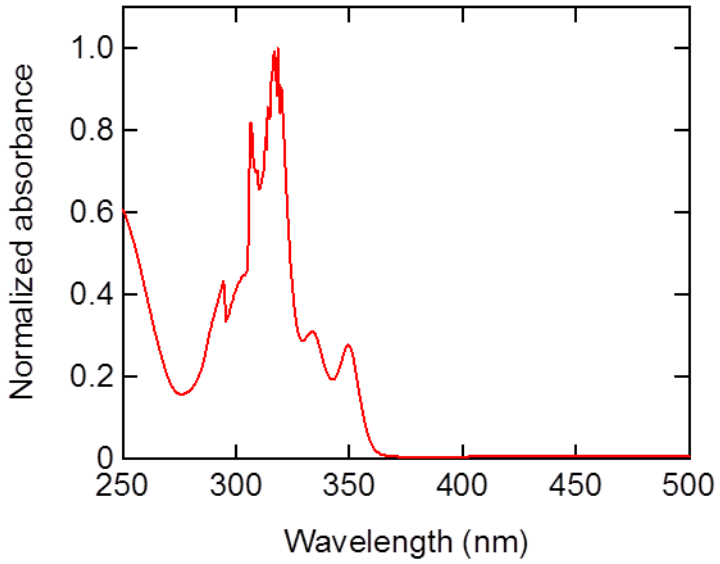

Figure S1. UV-Vis spectrum of DMeO-BTBT.

Electrochemical properties

Oxidation potentials were measured by cyclic voltammetry on an ALS model 701E electrochemical analyzer using chloroform as the solvent and $Bu_4N{\cdot}PF_6$ as the electrolyte (Fig. S2). The working electrode was glassy carbon, and the counter electrode was platinum. An oxidation potential of E_{onset} = 0.82 V was calculated from the average of three measurements with different sweep rates (100 mV/s, 50 mV/s, and 20 mV/s). HOMO energy level of E_{HOMO} = –5.57 eV was calculated by assuming the energy level of ferrocene to be –4.75 eV.

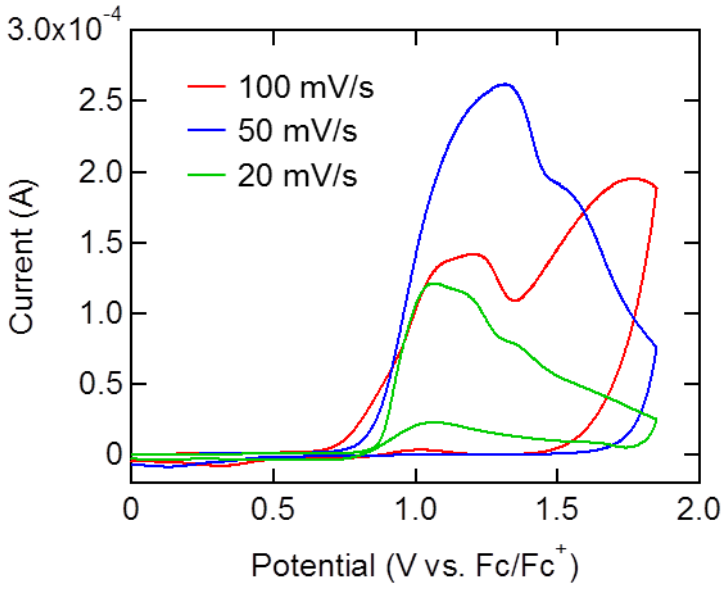

Figure S2. Cyclic voltammogram of DMeO-BTBT.

Single crystal structure

Single crystals of DMeO-BTBT were grown by recrystallization from ethyl acetate. Single crystals of (DMeO-BTBT)(TCNQ), (DMeO-BTBT)(F_2-TCNQ), and (DMeO-BTBT)(F_4-TCNQ) were grown by the diffusion method using an H-cell in dehydrated acetonitrile. DMeO-BTBT was added in a side of an H-cell, and F*n*-TCNQs was added in another side. Solvent was added slowly, and after a few days black needle-like crystals were harvested. Single-crystal X-ray structure analyses were carried out for (DMeO-BTBT)(TCNQ), (DMeO-BTBT)(F_2-TCNQ), and (DMeO-BTBT)(F_4-TCNQ) on a Rigaku AFC7R four-circle diffractometer at room temperature. The structures were solved by the direct method (SIR 2008) and refined by the full-matrix least-squares method by applying anisotropic temperature factors for all non-hydrogen atoms using the SHELX-97 programs.[S1,S2] The hydrogen atoms were placed at geometrically calculated positions. The intermolecular transfer integrals t_i between donor HOMOs were calculated from the intermolecular overlaps of HOMO obtained from the MOPAC, AM1 molecular orbital calculation.[S3,S4] Crystals for thin-film and single-crystal transistors were grown by the recrystallization in acetonitrile, because crystals grown by the diffusion method is insufficient for vacuum evaporation in quantity and too large for the single-crystal transistors.

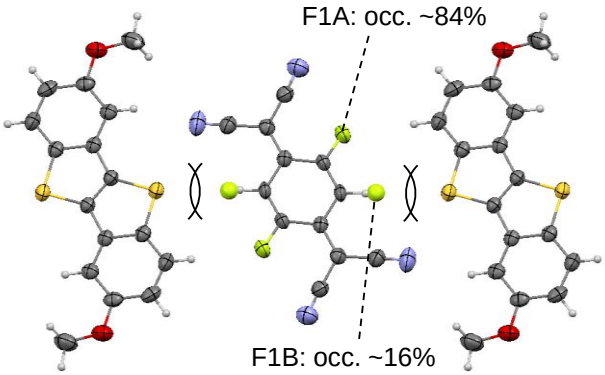

Figure S3. The positional disorder of the fluorine atoms on F_2-TCNQ.

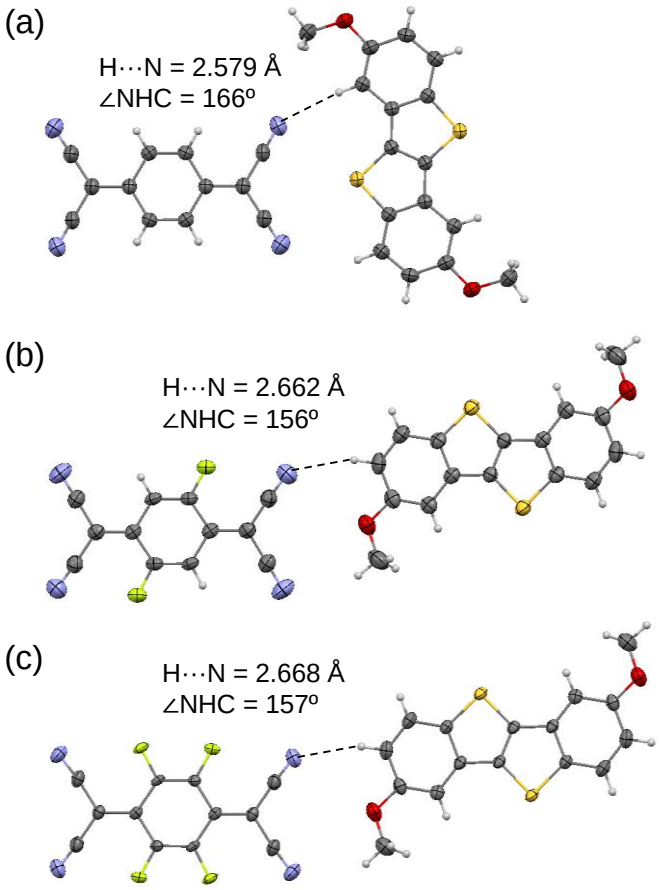

Figure S4. The C−H···N hydrogen bond patterns in (a) (DMeO-BTBT)(TCNQ), (b) (DMeO)-BTBT)(F_2-TCNQ), and (c) (DMeO-BTBT)(F_4-TCNQ).

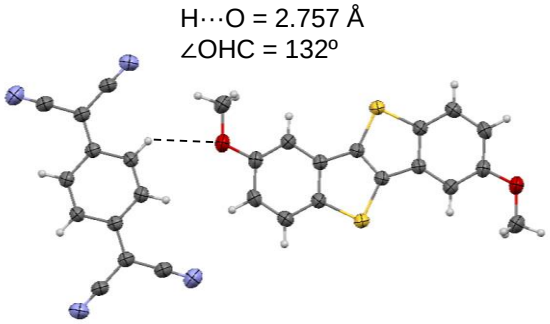

Figure S5. The C–H···O hydrogen bond pattern in (DMeO-BTBT)(TCNQ).

Degree of charge transfer

In order to investigate the charge transfer degree in the CT complexes, bond lengths of the TCNQ derivatives are listed in Table S1 together with those of the neutral molecules. The following formulas have been proposed as the relation between the charge and the bond lengths,

$q_1 = 7.25(b - c) - 8.07(c - d) - 1$ [S8]

$q_2 = 22.42 - 23.81[(a + c)/(b + d)]$ [S9]

$q_3 = 26.28 - 27.94[(a + c)/(b + d)]$ [S10]

$q_4 = A - B[c/(b + d)]$ [S11]

where A = 19.818 and B = 41.667 for TCNQ, and A = 21.846 and B = 45.756 for F_4-TCNQ. Here a, b, c, and d are bond lengths listed in Table S1, and q is the (negative) charge on TCNQ. The estimated charge q is at most –0.2, but systematic changes to F_2-TCNQ and F_4-TCNQ are not observed. There is certain small charge transfer, but these CT complexes are essentially recognized as neutral complexes.

Table S1. Bond lengths and the estimated charges of the TCNQ derivatives in the neutral molecules and the DMeO-BTBT complexes.

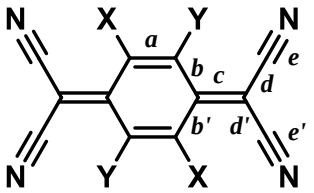

X = Y = H: TCNQ
X = F, Y = H: F_2-TCNQ
X = Y = F: F_4-TCNQ

	TCNQ†		F_2-TCNQ§		F_4-TCNQ†	
	neutral[S5]	complex	neutral[S6]	complex	neutral[S7]	complex
a	1.3462	1.345(2)	1.3281	1.342(7)	1.3336	1.350(8)
b	1.4453	1.440(2)	1.4394	1.435(5)	1.4355	1.438(5)
b′	1.4503	1.437(2)	1.4432	1.440(7)	1.4379	1.438(7)
c	1.3739	1.383(2)	1.3757	1.385(7)	1.3721	1.382(8)
d	1.4404	1.432(2)	1.4366	1.439(7)	1.4350	1.451(9)
d′	1.4415	1.427(2)	1.4368	1.428(6)	1.4394	1.436(9)
e	1.1386	1.136(2)	1.1356	1.128(8)	1.1384	1.145(9)
e′	1.1404	1.144(3)	1.1379	1.145(7)	1.1418	1.131(7)
q_1	0.077	–0.22(3)	–0.032	–0.23(10)	–0.006	–0.10(12)
q_2	0.010	–0.22(3)	0.061	–0.19(11)	0.014	–0.14(13)
q_3	–0.029	–0.30(4)	0.031	–0.26(13)	–0.025	–0.21(15)
q_4	0.001	–0.27(4)	-	-	0.043	–0.06(14)

† Average values for the equivalent bonds.

§ Average values of the non-equivalent bonds are used for *b*(*b′*) and *d*(*d′*).

Effective transfer integrals

The electronic coupling between donor (acceptor) molecules along the stacking direction are obtained using an energy-splitting approach by considering the energy levels of a D-A-D or A-D-A triad,

$$t_{\mathrm{h[e]}}^{\mathrm{eff}} = \frac{E_{\mathrm{H[L+1]}} - E_{\mathrm{H-1[L]}}}{2}$$

where $E_{\mathrm{H[L]}}$ and $E_{\mathrm{H-1[L+1]}}$ are the energies of the HOMO and HOMO−1 [LUMO and LUMO+1] levels taken from the neutral state of the D-A-D [A-D-A] triad. These calculations were performed with the B3LYP functional and 6-31G(d,p) basis set, using the Gaussian 03 package. In (DMeO-BTBT)(TCNQ), $t_{\mathrm{h}}^{\mathrm{eff}}$ and $t_{\mathrm{e}}^{\mathrm{eff}}$ are almost comparable, whereas in the F_2-TCNQ and F_4-TCNQ complexes, $t_{\mathrm{e}}^{\mathrm{eff}}$ is about three times larger than $t_{\mathrm{h}}^{\mathrm{eff}}$. This is attributed to the strong acceptor ability as well as the difference of the parallel and perpendicular molecular arrangements.

(a) D-A-D

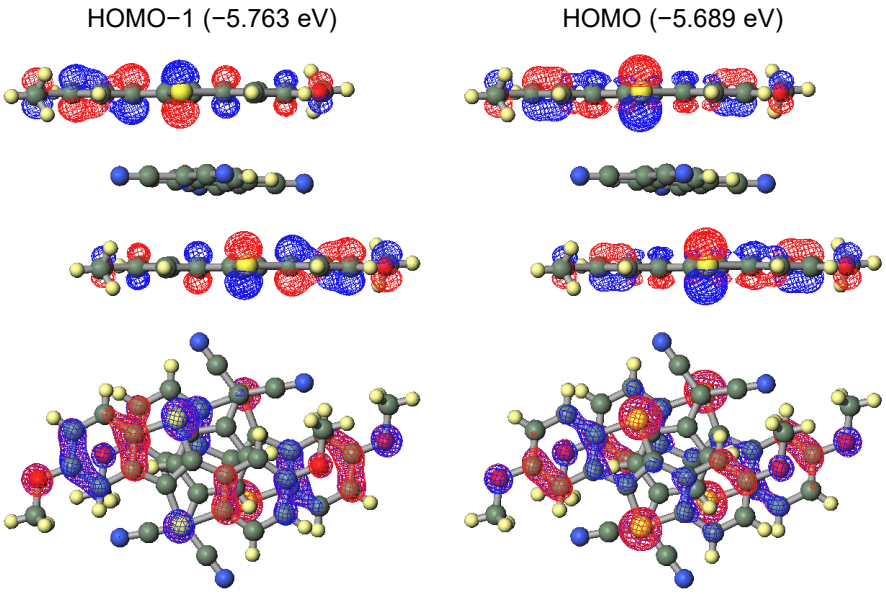

$t_h = (E_H - E_{H-1})/2 = 37$ meV

(b) A-D-A

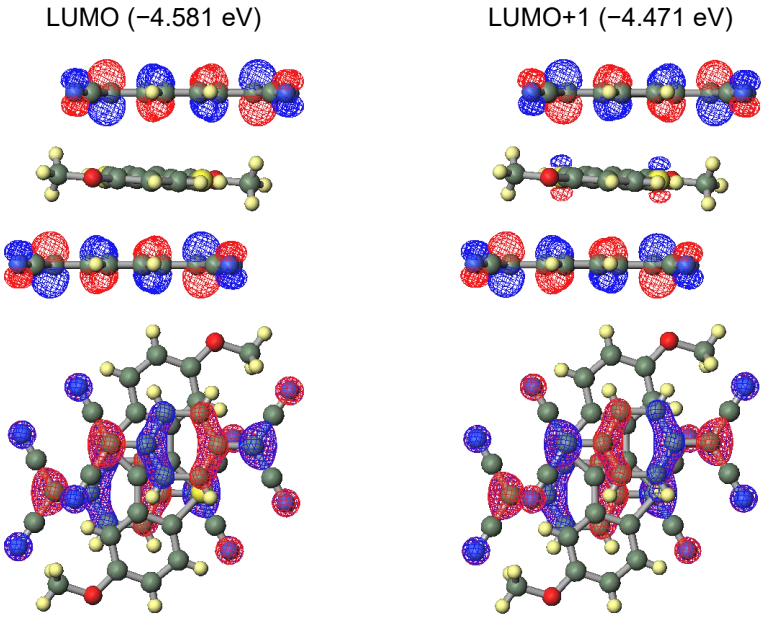

$t_e = (E_{L+1} - E_L)/2 = 55$ meV

Figure S6. Energy-splitting estimation of the transfer integrals along the stacking direction in the (DMeO-BTBT)(TCNQ) crystal: (a) holes and (b) electrons.

(a) D-A-D

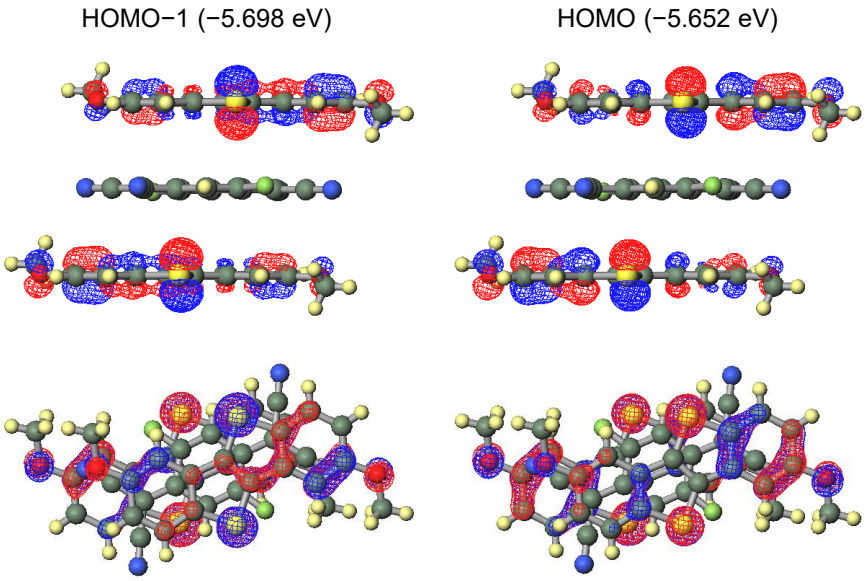

$t_h = (E_H - E_{H-1})/2 = 23$ meV

(b) A-D-A

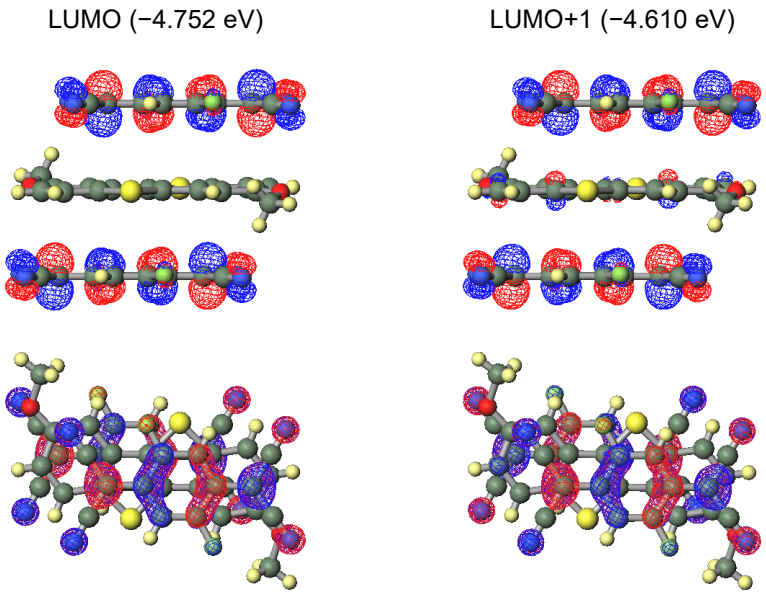

$t_e = (E_{L+1} - E_L)/2 = 71$ meV

Figure S7. Energy-splitting estimation of the transfer integrals along the stacking direction in the (DMeO-BTBT)(F_2-TCNQ) crystal: (a) holes and (b) electrons.

(a) D-A-D

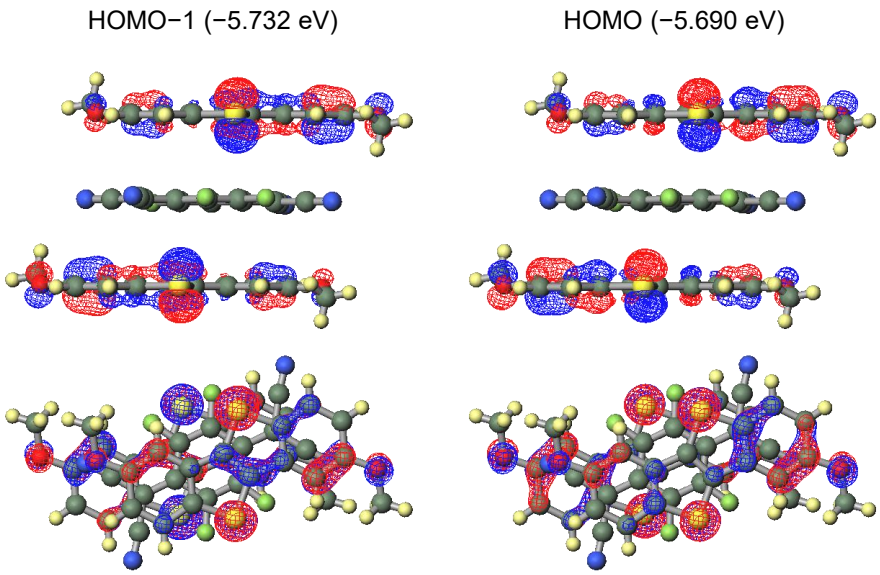

$t_h = (E_H - E_{H-1})/2 = 21$ meV

(b) A-D-A

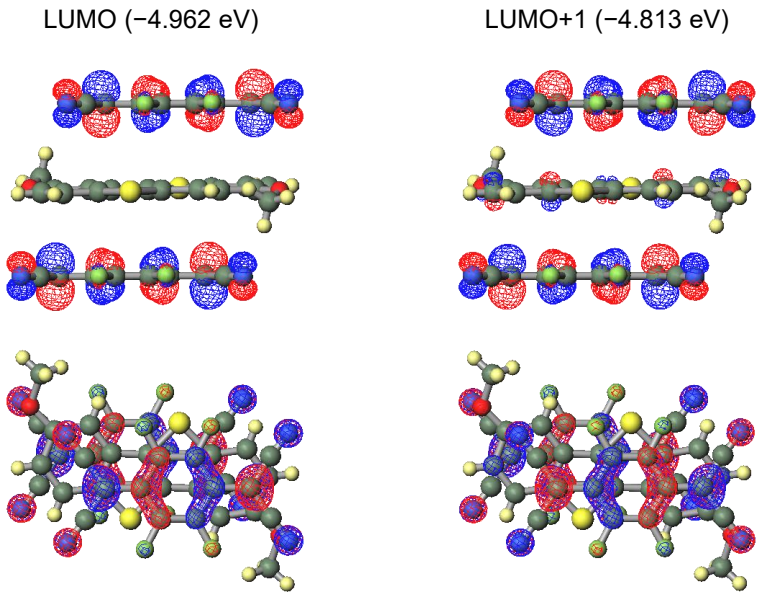

$t_e = (E_{L+1} - E_L)/2 = 75$ meV

Figure S8. Energy-splitting estimation of the transfer integrals along the stacking direction in the (DMeO-BTBT)(F_4-TCNQ) crystal: (a) holes and (b) electrons.

Device fabrication

Thin-film transistors were fabricated onto n-doped Si substrates with a thermally grown SiO_2 dielectric layer (300 nm, C = 11.5 nF/cm^2). For the thin-film device, the passivation layer tetratetracontane ($C_{44}H_{90}$, TTC, ε = 2.5) was evaporated under a vacuum of 10^{-3} Pa on the substrates with a thickness of 20 nm,[20] where the resulting overall capacitance of the gate dielectrics was 10.4 nF/cm^2.[S12] Then the charge-transfer salt with a thickness of 50 nm was vacuum evaporated. The top-contact electrodes were patterned by thermal deposition of (TTF)(TCNQ) using a shadow mask; the channel length (L) and width (W) were 100 μm and 1000 μm, respectively.

For the single-crystal device, the polystyrene (PS, ε = 2.5, 100 nm) layer was deposited by spin coating (3000 rpm, and 30 sec) from a solution of PS (20 mg) in toluene (1 mL) on the silicon surface,[S13] where the resulting overall capacitance was 7.6 nF/cm^2. Needle-like black crystals recrystallized from an acetonitrile solution were put on the PS layer using ethanol. Carbon paste (DOTITE, XC-12) was deposited on two ends of the single crystal to make the source-drain electrodes; the photographs with the channel lengths (L) and widths (W) are shown in Fig. S11. The transistor characteristics were measured under the vacuum of 10^{-4} Pa and ambient conditions just after the fabrication, by using a Keithley 4200 semiconductor parameter analyzer. The mobility was evaluated from the transconductance in the saturated region.

Transistor properties

Transfer and output characteristics of the thin-film transistors are shown in Fig. S9. The device performance is summarized in Table 3. n-Channel operation is observed for all cases both in vacuum and in air. However, in air the threshold voltages (V_{th}) are shifted and the mobility is reduced to some extent (Table 3). In particular, thin-film transistors of (DMeO-BTBT)(TCNQ) is not very air stable.

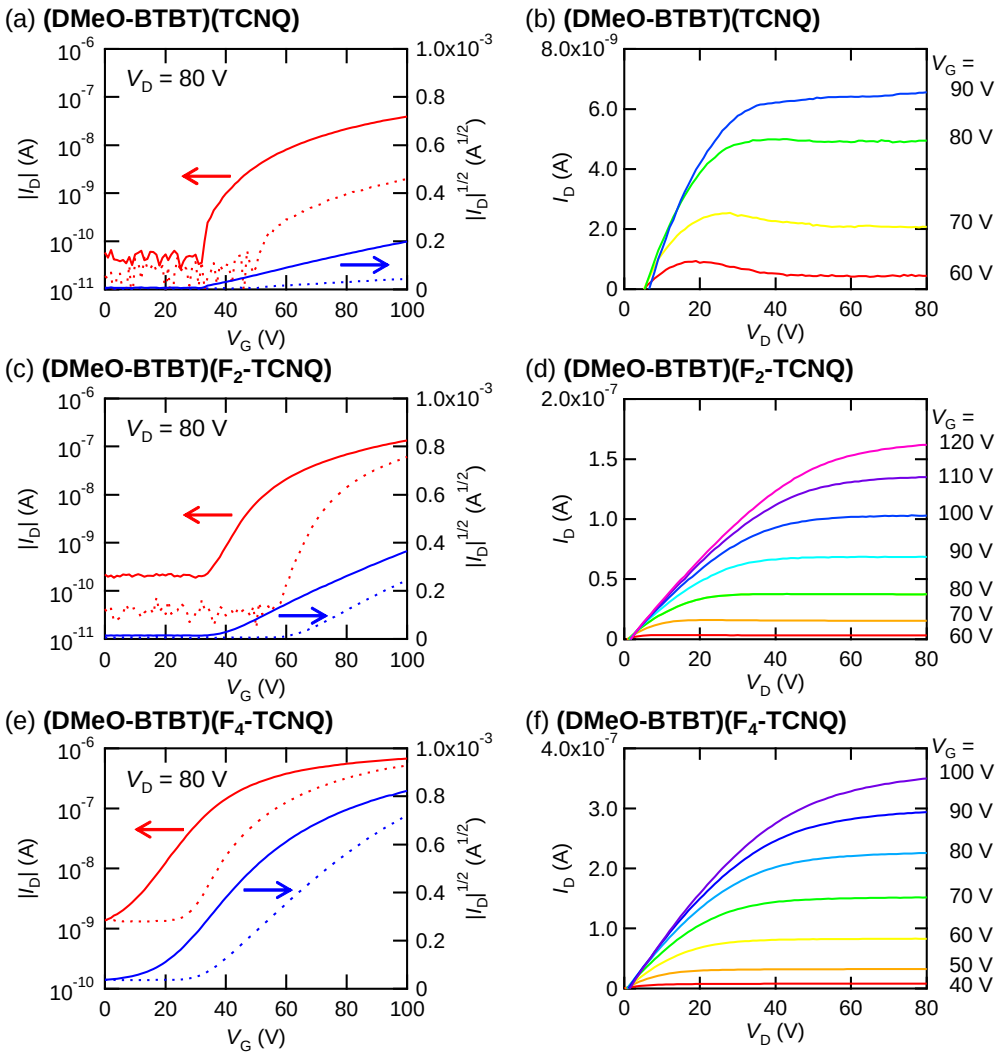

Figure S9. Typical transfer and output characteristics of thin-film transistors of (DMeO-BTBT)(F_n-TCNQ) (n = 0, 2, and 4). (a, b): n = 0, (c, d): n = 2, and (e, f): n = 4. The solid transfer characteristics are measured in vacuum and the dotted characteristics in air.

The durability of the single-crystal and thin-film transistors are shown in Fig. S10, and the transistor characteristics are summarized in Table 3. n-Channel operation is observed in air even after one year storage.

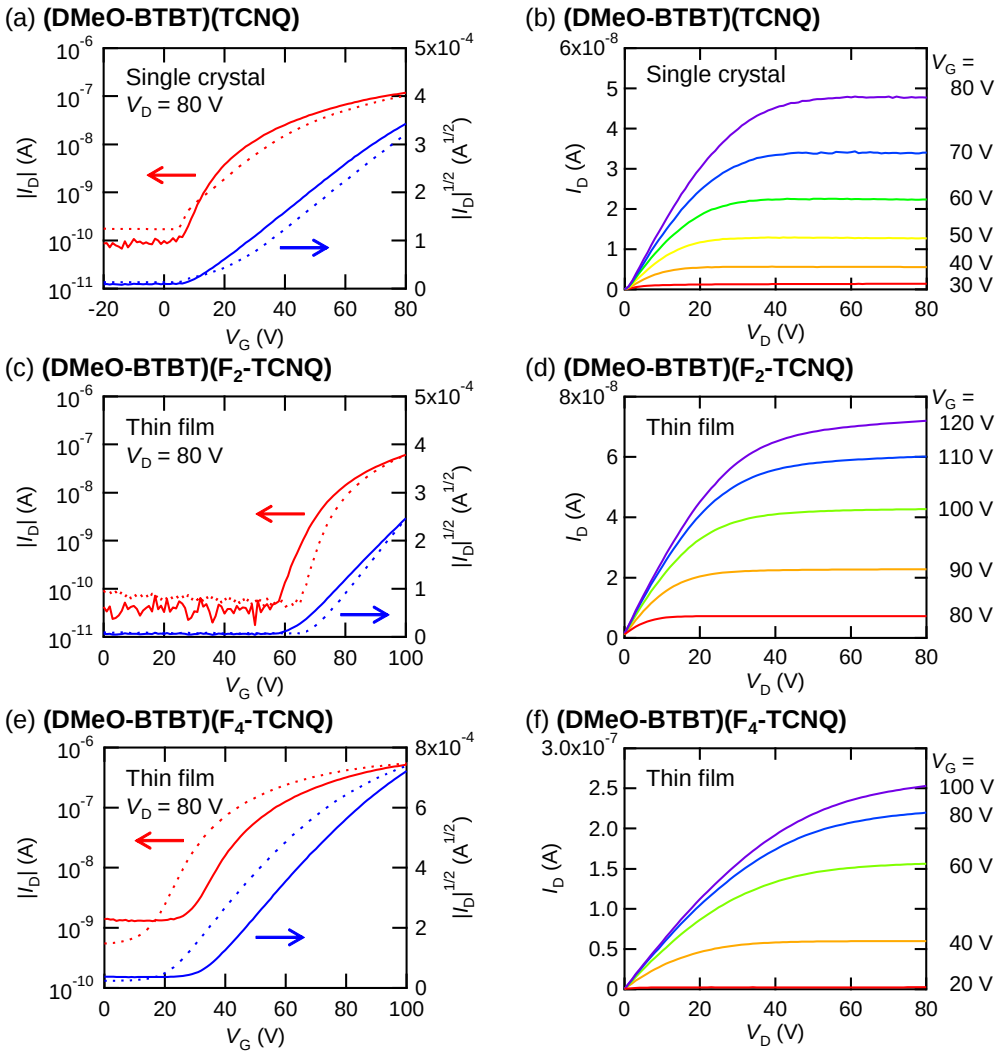

Figure S10. Typical transfer and output characteristics of single-crystal and thin-film transistors of (DMeO-BTBT)(F_n-TCNQ) (n = 0, 2, and 4). (a, b): n = 0, (c, d): n = 2, and (e, f): n = 4. The solid transfer characteristics are measured in air and the dotted characteristics are measured in air after one-year storage.

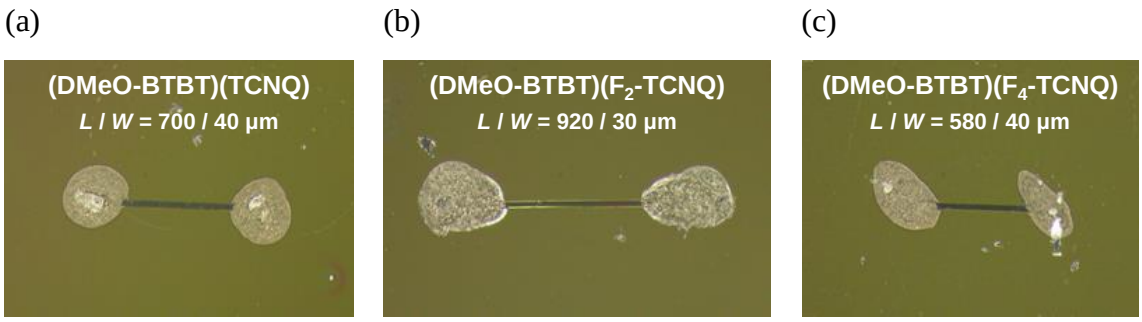

Figure S11. The photographs with the channel lengths (*L*) and widths (*W*) of the single-crystal transistors of (a) (DMeO-BTBT)(TCNQ), (b) (DMeO-BTBT)(F_2-TCNQ) and (c) (DMeO-BTBT)(F_4-TCNQ).

References

[S1] M. C. Burla, R. Caliandro, M. Camalli, B. Carrozzini, G. L. Cascarano, L. de Caro, C. Giacovazzo, G. Polidori, D. Siliqi and R. Spagna, *J. Appl. Crystallogr*., 2007, **40**, 609.

[S2] G. M. Sheldrick, *Acta Crystallogr*., *Sect. A: Found. Crystallogr*., 2008, **A64**, 112.

[S3] T. Mori, A. Kobayashi, Y. Sasaki, H. Kobayashi, G. Saito and H. Inokuchi, *Bull. Chem. Soc. Jpn*., 1984, **57**, 627.

[S4] M. J. S. Dewar, E. G. Zoebisch, E. F. Healy and J. J. P. Stewart, *J. Am. Chem. Soc*., 1985, **107**, 3902.

[S5] R. E. Long, R. A. Sparks and K. N. Trueblood, *Acta Cryst.*, 1965, **18**, 932.

[S6] F. M. Wiygul, J. P. Ferraris, T. J. Emge and T. J. Kistenmacher, *Mol. Cryst. Liq. Cryst.*, 1981, **78**, 279.

[S7] T. J. Emge, M. Maxfield, D. O. Cowan and T. J. Kistenmacher, *Mol. Cryst. Liq. Cryst.*, 1981, **65**, 161.

[S8] S. Flandrois and D. Chasseau, *Acta Crystallogr., Sect. B: Struct. Crystallogr. Struct. Chem.*, 1977, **B33**, 2744.

[S9] P. Coppens and T. N. Guru Row, *Ann. N.Y. Acad. Sci.*, 1978, **313**, 244.

[S10] T. C. Umland, S. Allie, T. Kuhlmann and P. Coppens, *J. Phys. Chem.*, 1988, **92**, 6456.

[S11] A. L. Sutton, B. F. Abrahams, D. M. D'Alessandro, R. W. Elliott, T. A. Hudson, R. Robson and P. M. Usov, *CrystEngComm*, 2014, **16**, 5234.

[S12] K.-J. Baeg, Y.-Y. Noh, J. Ghim, B. Lim and D.-Y. Kim, *Adv. Funct. Mater.*, 2008, **18**, 3678.

[S13] M.-H. Yoon, H. Yan, A. Facchetti and T. J. Marks, *J. Am. Chem. Soc*., 2005, **127**, 10388.